THE JOURNAL OF PHYSICAL CHEMISTRY C

Article

pubs.acs.org/JPCC

A Processing Window for Fabricating Heavily Doped Silicon Nanowires by Metal-Assisted Chemical Etching

Yangyang Qi, Zhen Wang, Mingliang Zhang, Fuhua Yang, and Xiaodong Wang*

Engineering Research Center for Semiconductor Integrated Technology, Institute of Semiconductors, Chinese Academy of Sciences, Beijing 100083, China

ABSTRACT: Heavily doped silicon nanowires (SiNWs) with controllable doping concentrations can be used in many fields because of their unique characteristics. However, it is difficult to fabricate long heavily doped SiNWs. In this article, a systematic study of metal-assisted chemical etching (MACE) of heavily doped silicon wafers is presented. High-quality SiNWs with lengths up to 40 μm could be achieved. The electron-transfer processes among Si, Ag^+, Ag nanoparticles, and H_2O_2 were investigated to explain the formation of SiNWs. A chemical etching processing window, considering HF and H_2O_2 concentrations, reaction temperature, and etching time, is proposed. To obtain SiNWs, the etching reaction should occur at room temperature for less than 40 min. The appropriate concentration ranges are 0.2−0.4 M for H_2O_2 and 8−10 M for HF. Transmission electron microscopy (TEM) measurements confirmed that the as-prepared nanowires were single-crystalline. Current−voltage (I−V) measurements of an individual nanowire showed a resistance larger than the calculated value based on bulk silicon. This work can provide guidelines for obtaining high-quality heavily doped SiNWs using the MACE method.

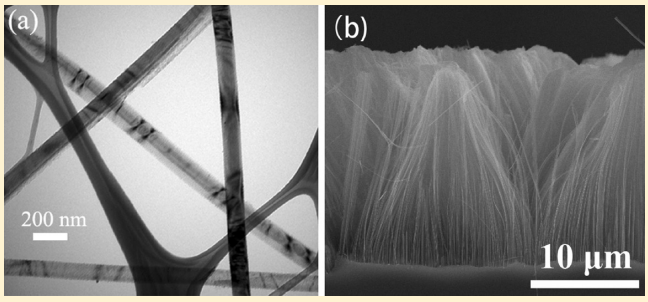

1. INTRODUCTION

Heavily doped silicon nanowires (SiNWs) with controllable hole or electron doping concentrations are attractive building blocks in the fields of thermoelectrics,[1] nanoelectronics,[2,3] photovoltaics,[4] and battery electrodes.[5,6] It has been reported that heavily doped SiNWs have a thermoelectric figure of merit of 0.6, which is nearly 2 orders of magnitude larger than that of bulk silicon,[7] indicating that heavily doped SiNWs are effective thermoelectric materials. Heavily doped porous SiNWs loaded with platinum nanoparticles (NPs) can be used as effective photocatalysts for the photocatalytic degradation of organic dyes and toxic pollutants under visible irradiation.[8] To satisfy the demand for SiNWs, controllable and large-scale fabrication of heavily doped SiNWs is required. Because of its low costs and wafer-scale fabrication, metal-assisted chemical etching (MACE) is an attractive fabrication method,[9−11] and the resulting nanowires retain the single-crystalline structure of the starting silicon wafer.[12,13]

Compared with lightly doped SiNWs, it is quite challenging to obtain high-quality heavily doped SiNWs with the desired lengths using the MACE method. Figure 1 shows the scanning electron microscopy (SEM) results of experiments in which lightly doped (resistivity of 3−7 Ω·cm) and heavily doped (resistivity of <0.0035 Ω·cm) silicon substrates were etched under the same conditions, namely, in a mixture of 8.5 M HF and 0.6 M H_2O_2 at room temperature (25 °C) for 2 h. It was found that lightly doped SiNWs were obtained with a good morphology (Figure 1a,b). They were well separated and had a length of about 60 μm. However, the SiNWs from the heavily doped silicon substrate showed an overetched feature (Figure

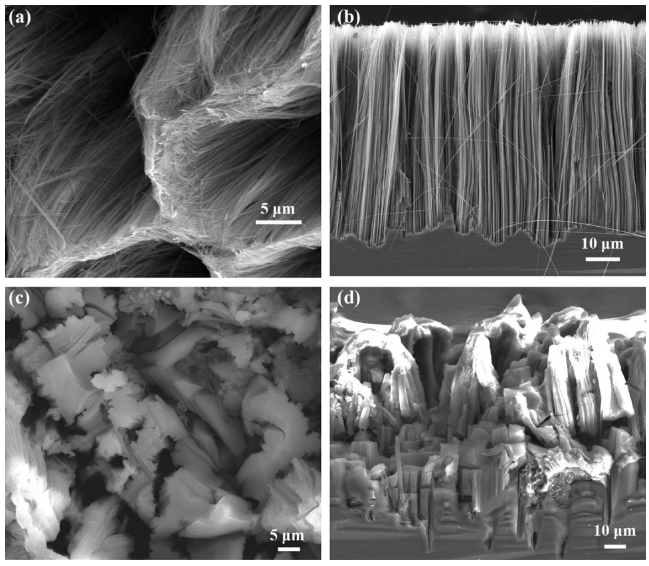

Figure 1. (a,c) Top-view and (b,d) cross-sectional SEM images of SiNWs formed on silicon substrates with resistivities of (a,b) 3−7 and (c,d) <0.0035 Ω·cm. Note that the etching reaction occurred under the same conditions, namely, in a solution containing 8.5 M HF and 0.6 M H_2O_2 at room temperature for 2 h.

Received: August 2, 2013
Revised: October 25, 2013
Published: October 29, 2013

1c,d), which indicated that the heavily doped SiNWs are more sensitive to the etching conditions. Therefore, it is necessary to find the proper etching conditions for fabricating long and high-quality heavily doped SiNWs.

In this work, the effects of H_2O_2 concentration (0.2−2 M), HF concentration (5−11 M), reaction temperature (10−40 °C), and reaction time (10−60 min) on the morphology of SiNWs were studied. A chemical etching processing window, including these parameters, was determined. The cause of this processing window is discussed based on the electron transfer among Si, Ag^+, Ag NPs, and H_2O_2. To obtain high-quality heavily doped SiNWs, the chemical reaction should be controlled at room temperature for less than 40 min. The appropriate H_2O_2 and HF concentrations were found to be 0.2−0.4 and 8−10 M, respectively. The resulting SiNWs were characterized by SEM, transmission electron microscopy (TEM), and current−voltage (I−V) measurements. The results confirmed that the high-quality SiNWs obtained with lengths of up to 40 μm were single-crystalline and had a larger resistance than bulk Si.

2. EXPERIMENTAL SECTION

A commercial silicon wafer, n-type with crystal orientation (100) and <0.0035 Ω·cm resistivity, acted as the starting material. First, it was cut into 1 × 1 cm^2 squares and washed using H_2SO_4 (95−98%) and H_2O_2 (30%) in a volume ratio 3:1 for 15 min. Then, the sample was immersed in dilute HF to remove the thin oxide layer. A hydrogen-terminated surface was obtained. Second, the sample surface was covered with Ag NPs by immersing the wafer in a solution containing 0.005 M $AgNO_3$ and 5 M HF for about 2 min at room temperature. After the excess Ag^+ had been removed using deionized water, the sample was put into an etching solution composed of HF and H_2O_2. An anisotropic etching process took place. At the end of the etching reaction, HNO_3 was used to dissolve the Ag NPs for 10 min, and then dilute HF was used to remove SiO_2 from the surface of the SiNWs. Various etchant concentrations, reaction temperatures, and etching times were employed to study their effects on the etching. The relationships between these key parameters and the properties of the SiNWs were mainly investigated by SEM using a Hitachi S-4800 system. The crystalline quality of the SiNWs was analyzed by TEM. I−V measurements of an individual nanowire were performed using an Agilent B1500A semiconductor analyzer, and the sample was loaded on a Lakeshore CR6-4K probe stage.

3. RESULTS AND DISCUSSION

3.1. Mechanism for the Formation of SiNW Arrays. The etching of a Si wafer in a solution containing HF and H_2O_2 is a redox reaction. To clarify the formation mechanism of SiNWs, the properties of Si, Ag^+, Ag, and H_2O_2 in HF solution should be understood. A semiquantitative energy diagram (Scheme 1) shows the potential distribution of Si, Ag^+, Ag, and H_2O_2 in HF solution. The band edge bends at the interface of Si and etching solution.[14] The energy is referred to the standard hydrogen electrode potential. The energies of the valence band (E_{VB}) and conduction band (E_{CB}) of Si are 0.62 and −0.48 eV, respectively.[15] $E_{Ag^+/Ag}$ and $E_{H_2O_2/H_2O}$ represent the potential energies of the redox pairs Ag^+/Ag and H_2O_2/H_2O, which are 0.79 and 1.78 V, respectively.[16] E_{Ag^+} and E_{Ag} are the estimated potential energies of Ag^+ and Ag, respectively, and schematically represented in Scheme 1.[15] Because the Fermi energy (E_F) of n-type Si is more negative than the redox potential $E_{H_2O_2/H_2O}$, electrons preferentially transport from Si to H_2O_2. Ag acts as a catalyst and accelerates the redox reaction. Equations 1−3 simply describe the electron transport from Si to H_2O_2.[16,17]

Scheme 1. Semiquantitative Energy Diagram of Si, Ag^+/Ag, and H_2O_2/H_2O Redox Pairs[a]

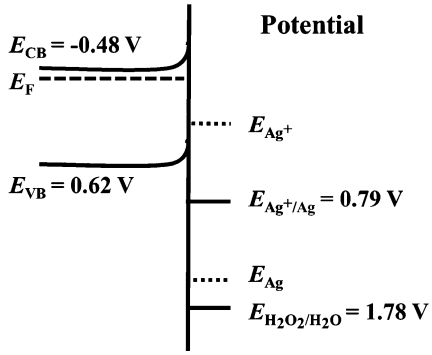

[a]Energy is referred to the standard hydrogen electrode potential.

$$Si + 6F^- \rightarrow [SiF_6]^{2-} + 4e^- \quad E_0 = 1.24\ V \tag{1}$$

$$Ag^+ + e^- \rightarrow Ag \quad E_0 = 0.79\ V \tag{2}$$

$$H_2O_2 + 2H^+ + 2e^- \rightarrow 2H_2O \quad E_0 = 1.78\ V \tag{3}$$

Electrons at E_F need to overcome the excitation barrier and band-edge bending to reach E_{Ag^+}.[15] Si loses electrons and is dissolved by HF as described by eq 1. Ag^+ obtains electron and is reduced to Ag as shown in eq 2. Because the redox potential $E_{H_2O_2/H_2O}$ is more positive than $E_{Ag^+/Ag}$, H_2O_2 captures electrons from Ag and is reduced to H_2O, and Ag is oxidized to Ag^+, which will subsequently take part in the oxidation process of Si. With increasing doping concentration of Si wafer, E_F shifts toward E_{CB}, and the space charge layer induced by band-edge bending is squeezed. In this case, electrons have more chances to overcome the excitation barrier and tunnel at the space charge layer, which explains why the MACE of heavily doped Si wafer is violent, as shown in Figure 1c,d. The total etching reaction can be described as[17]

$$Si + 6F^- + 2H_2O_2 + 4H^+ \rightarrow 4H_2O + SiF_6^{2-} \tag{4}$$

The Nernst equation for the net reaction is

$$E = 3.02\ V + \frac{0.0591}{4}\left(\log \frac{[H_2O_2]^2[H^+]^4[F^-]^6}{[SiF_6^{2-}]}\right) \tag{5}$$

where E is the reaction potential. According to the Nernst equation, with increasing concentration of H_2O_2 and HF, the reaction potential becomes great, and the etching rate increases. However, the etching rate cannot increase infinitely, and an appropriate range of etchant concentration should be chosen for the formation of high-quality SiNWs.

3.2. Effects of H_2O_2 and HF Concentrations. The effects of the H_2O_2 concentration were investigated in the range of 0.2−2 M at constant conditions of 8 M HF and 25 °C. The top-view images of the as-prepared SiNWs at different H_2O_2 concentrations are shown in Figure 2a−c. When the H_2O_2 concentration was 0.2 M, as shown in Figure 2a, well-separated nanowires with small diameters were observed. When the H_2O_2 concentration was increased to 0.4 M (Figure 2b), some

dx.doi.org/10.1021/jp407720e | J. Phys. Chem. C 2013, 117, 25090−25096

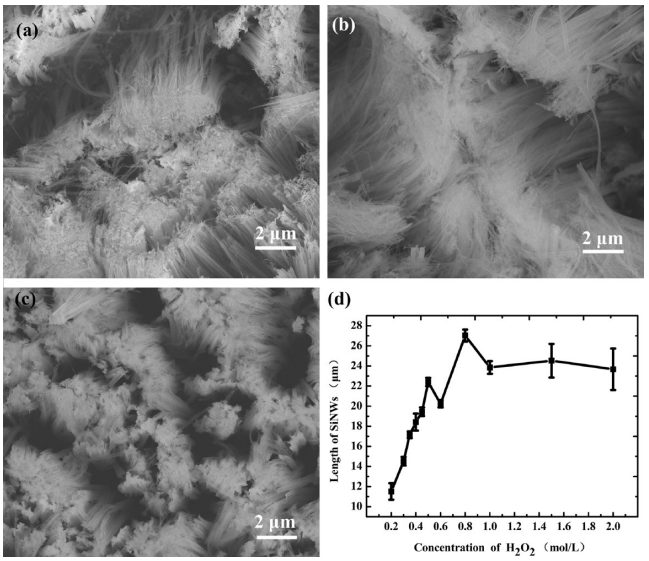

Figure 2. Top-view SEM images of the as-prepared SiNWs formed in solutions containing 8 M HF and (a) 0.2, (b) 0.4, and (c) 0.6 M H_2O_2 for 15 min at 25 °C. (d) Length evolution of the SiNWs as a function of H_2O_2 concentration.

flocculent structures appeared at the tips of the nanowires. A further increase in H_2O_2 concentration, for example, to 0.6 M as shown in Figure 2c, obviously produced nanowires with large diameters. The tips of these nanowires congregated, which can be attributed to the high etching rate. As shown in Figure 2d, when the H_2O_2 concentration was 0.6 M, the etching rate was 1.47 μm/min, which was clearly higher than the rates at H_2O_2 concentrations of 0.2 and 0.4 M. The high etching rate resulted in long nanowires, which easily collapsed and came together. In addition, in the solutions with high H_2O_2 concentrations, more Ag NPs were oxidized to Ag^+. These Ag^+ ions diffused upward and nucleated on the sidewall or tip of the SiNWs.[17] These new deposit sites were subsequently etched, leading to disorder of the SiNW array.

The length evolution of the SiNWs as a function of H_2O_2 concentration is shown in Figure 2d. A nonmonotonic curve was obtained. The maximum etching rate was realized when the H_2O_2 concentration was 0.8 M. At the first increasing stage, that is, for H_2O_2 concentrations from 0.2 to 0.8 M, the etching rate increased from 0.8 to 1.8 μm/min, indicating that the etching rate depended strongly on the H_2O_2 concentration.[13] When the concentration of H_2O_2 was low, only a few Ag NPs were oxidized to Ag^+ ions, which were able to obtain electrons from Si, so that Si was oxidized. The rate of Si oxidation was limited by the small amount of Ag^+. At the same time, the resulting oxide of Si could be dissolved in a timely manner by HF. In other words, the oxidation rate of Si was lower than the dissolution rate at this stage. With increasing H_2O_2 concentration, more Ag NPs were oxidized to Ag^+. The oxidation rate increased and gradually approached the dissolution rate. When the H_2O_2 concentration was increased to 0.8 M, the oxidation rate was equal to the dissolution rate, and the etching rate reached a maximum. When the H_2O_2 concentration was higher than 0.8 M, the length of SiNWs remained constant, as shown in Figure 2d, indicating that the etching rate did not increase with the H_2O_2 concentration. Three reasons for this behavior were considered here. The first was that an excessively high H_2O_2 concentration produced excess Ag^+, which could not be reduced in a timely manner by the Si at the root of SiNWs. Some of the excess Ag^+ diffused upward and nucleated at the sidewall of the SiNWs, which was apt to occur on the heavily doped Si wafer because of its higher defect state.[17] As a result, the Ag NPs at the root of the nanowires became smaller. The vertical etching rate decreased. The second reason was that, when the H_2O_2 concentration surpassed 0.8 M, the oxidation rate was higher than the dissolution rate. An oxidation layer covered the surface of the Si and could not be dissolved in a timely manner by HF. This oxidation layer hindered the electron migration from Si to Ag^+, so the oxidation rate was limited. The oxidation and dissolution of Si achieved a balance. The third reason was that the long nanowires were too fragile to preserve the arrays. Part of the nanowires collapsed, which prevented the etchants from approaching the root of the nanowires. The etching rate decreased. In addition, SiNW arrays with inconsistent lengths were observed when the H_2O_2 concentration was higher than 1 M, indicating that the reaction became unstable. For example, when the H_2O_2 concentration was 1.5 M, the lengths of the SiNWs varied from 23 to 26 μm, as shown in Figure 2d. Therefore, H_2O_2 concentrations that are too high should be avoided. According to the experimental results, the appropriate H_2O_2 concentration was 0.2−0.4 M when the concentration of HF was kept at 8 M at room temperature.

The effects of the HF concentration were investigated in the range of 5−11 M at 0.4 M H_2O_2 and 25 °C. Panels a−c of Figure 3 show the SiNWs obtained in 7, 9, and 11 M HF,

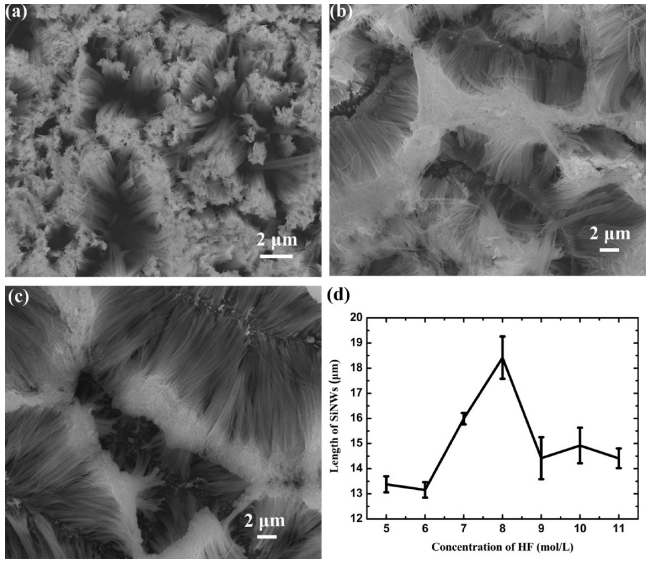

Figure 3. Top-view SEM images of the as-prepared SiNWs formed in solutions containing 0.4 M H_2O_2 and (a) 7, (b) 9, and (c) 11 M HF for 15 min at 25 °C. (d) Length evolution of the SiNWs as a function of HF concentration.

respectively. When the HF concentration was low (i.e., 7 M, as shown in Figure 3a), SiNWs with large diameters were observed. When the HF concentration was increased to 9 M (Figure 3b), the tips of the SiNWs gathered together to form clusters. When the HF concentration was increased further to 11 M (Figure 3c), the tips of the SiNWs became twisted, indicating that the tips were etched.

The length evolution of the SiNWs as a function of HF concentration is displayed in Figure 3d. When the HF

dx.doi.org/10.1021/jp407720e | J. Phys. Chem. C 2013, 117, 25090−25096

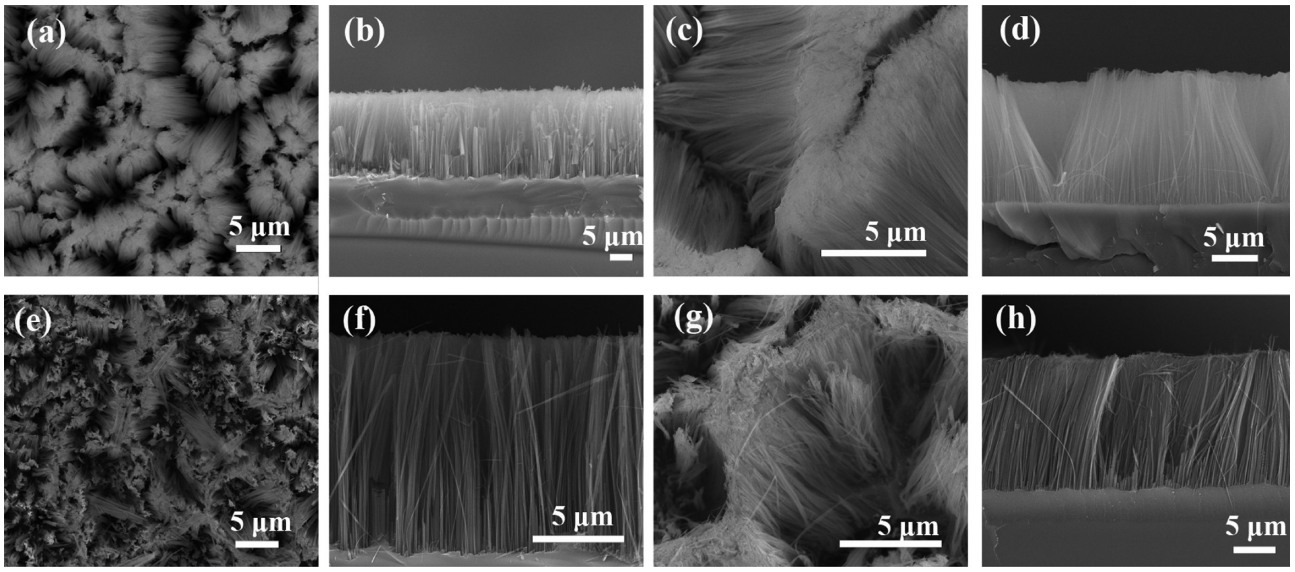

Figure 4. (a,c,e,g) Top-view and (b,d,f,h) cross-sectional SEM images of SiNWs formed in solutions containing (a,b) 0.4 M H_2O_2 and 8 M HF at 40 °C for 15 min, (c,d) 0.25 M H_2O_2 and 8 M HF at 40 °C for 15 min, (e,f) 0.4 M H_2O_2 and 8 M HF at 10 °C for 15 min, and (g,h) 0.4 M H_2O_2 and 14 M HF at 10 °C for 15 min.

concentration was increased from 5 to 11 M, the length of the SiNWs first increased, then decreased, and finally remained constant, indicating that the evolution of the etching rate was nonmonotonic. The effects of the HF concentration on the morphology and length of the SiNWs can be explained by the electron-transfer processes among Si, Ag^+, Ag NPs, and H_2O_2. When the HF concentration was low, there was not enough HF to dissolve the oxide formed beneath the Ag NPs. This oxide layer hindered the electron transfer from Si to Ag^+. Therefore, the etching rate was low and restricted by HF. In this case, excess Ag^+ ions could not be reduced. They diffused upward and deposited on the sidewall of the SiNWs, which resulted in SiNWs with a rough surface and large diameter. With an increase in the HF concentration, the oxidation and dissolution rates of Si achieved a balance, and the etching rate reached a maximum. Further increasing the HF concentration could not accelerate the etching reaction, because the H_2O_2 concentration limited the Si oxidation rate. In addition, the etching occurred not only at the root but also at the tips of the SiNWs, which could be verified by the whisker-shaped structures at the tips of the SiNWs shown in Figure 3c. At the root of the nanowires, the etching solution must access the interface between Ag and silicon to etch the underlying Si. The increase of the etching depth resulted in less chance for HF to access the interface. The aggregation of the SiNWs shown in Figure 3b,c also affected the diffusion of the etching solution. Consequently, the etching rate at the root of the SiNWs decreased, whereas the etching rate at the tips was low and remained unchanged. When the HF concentration was increased to 9 M, the etching rate at the tips of nanowires was equal to that at the root. The length of the nanowires finally remained constant. Hence, there is no necessity to use a high HF concentration to obtain long nanowires. Based on the experimental results, the appropriate HF concentration is 8−10 M. Therefore, both the HF and H_2O_2 concentration had obvious impacts on the etching process. For MACE performed at 25 °C for 15 min, the appropriate H_2O_2 concentration was found to be 0.2−0.4 M, and the cooresponding appropriate HF concentration was 8−10 M.

3.3. Effects of Reaction Temperature. In addition to the normally used reaction temperature 25 °C, a similar etching process was performed at higher (40 °C) and lower (10 °C) temperatures to investigate the effects of temperature on the morphology and etching rate of SiNWs. At the normally used reaction temperature of 25 °C, it was found that concentrations of 0.4 M H_2O_2 and 8 M HF were appropriate for fabricating SiNWs. Therefore, these etchant concentrations were also used at 40 and 10 °C as preliminary values. The etching reaction was carried out for 15 min. The results are shown in Figure 4a,b,e,f. The length of SiNWs obtained at 40 °C was about 15 μm (Figure 4b), and that at 10 °C was about 10 μm (Figure 4f), indicating that the etching rate increased with etching temperature.[18] In addition, the etching temperature had an effect on the morphology of SiNWs. From Figure 4a,b, it can be seen that the SiNWs were overetched at 40 °C. Parts of the SiNWs were broken, indicating that the etching reaction was too violent. As shown in Scheme 1, when the temperature was high, electrons had more chances to overcome the excitation barrier and band-edge bending. The oxidation of Si occurred more easily. Moreover, high temperature could accelerate the diffusion of the etching solution, which could also enhance the etching rate. Therefore, the H_2O_2 concentration should be reduced appropriately to counteract the effect of temperature. Thus, not as many Ag NPs were oxidized to Ag^+, and the oxidation of Si was suppressed. According to the experimental results, the suitable range of H_2O_2 concentrations at 40 °C was 0.15−0.25 M, which was lower than the 0.2−0.4 M range obtained at 25 °C. Figure 4c,d shows the SiNWs formed under optimized etching conditions, that is, in a solution containing 0.25 M H_2O_2 and 8 M HF for 15 min. It can be seen that the SiNW array was ordered. At low temperature (10 °C), some SiNWs with large diameters were observed (see Figure 4e,f), because it was difficult for electrons to overcome the energy barrier at low temperature and the etching rate was low. Therefore, it was necessary to slightly increase the etchant concentrations to accelerate the reaction. The appropriate HF concentration was 10−14 M at 10 °C, which was higher than the 8−10 M used at 25 °C. The range of H_2O_2 concentrations

dx.doi.org/10.1021/jp407720e | J. Phys. Chem. C 2013, 117, 25090−25096

was 0.3−0.6 M. Figure 4g,h shows the higher-quality SiNWs formed in the solution containing 0.4 M H_2O_2 and 14 M HF. Compared with Figure 4e, SiNWs with larger diameters were hardly observed in Figure 4g.

3.4. Effects of Reaction Time. The dependence of the SiNW length on the reaction time was studied in the range from 15 to 60 min. As shown in Figure 5, for the solution

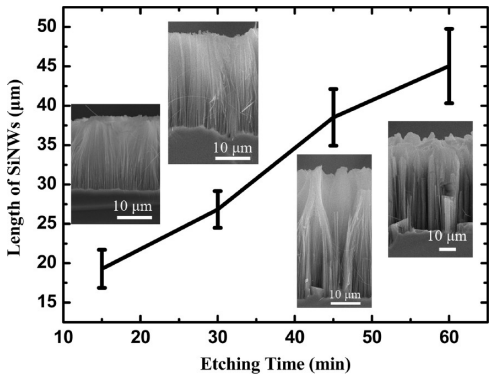

Figure 5. Length evolution of SiNWs as a function of etching time. The insets are cross-sectional SEM images of SiNWs synthesized for (from left to right) 15, 30, 45, and 60 min.

containing 0.4 M H_2O_2 and 8 M HF at 25 °C, the SiNW length exhibited a nearly linear relationship with the etching time. The etching rate was about 0.75 μm/min. The insets in Figure 5 are cross-sectional SEM images of SiNWs synthesized for 15, 30, 45, and 60 min. At 45 min, the tips of the SiNWs congregated. This aggregation of the tips hindered further etching reaction. At 60 min, it was obvious that the SiNWs had been overetched. Hence, to obtain high-quality SiNWs, the reaction time should be controlled at 40 min.

Based on the results mentioned above, a processing window for fabricating heavily doped SiNWs using the MACE method is summarized in Table 1. At 25 °C, the appropriate H_2O_2 and

Table 1. Suitable Parameters for Fabricating Heavily Doped SiNWs

temperature (°C)	H_2O_2 concentration[a] (M)	HF concentration[b] (M)	reaction time[c] (min)
10	0.3−0.6 (10 M HF)	10−14 (0.4 M H_2O_2)	<60 (10 M HF, 0.4 M H_2O_2)
25	0.2−0.4 (8 M HF)	8−10 (0.4 M H_2O_2)	<40 (8 M HF, 0.4 M H_2O_2)
40	0.15−0.25 (8 M HF)	7−9 (0.25 M H_2O_2)	<30 (8 M HF, 0.25 M H_2O_2)

[a]Suitable H_2O_2 concentration obtained for the specific HF concentration listed in parentheses. [b]Suitable HF concentration obtained for the specific H_2O_2 concentration listed in parentheses. [c]Suitable reaction time obtained for the specific H_2O_2 and HF concentrations listed in parentheses.

HF concentrations are 0.2−0.4 and 8−10 M, respectively. The etching time should be controlled at 40 min. At the lower temperature 10 °C, because the activity of the etchants decreases, the concentrations of etchants should be slightly increased. The suitable H_2O_2 and HF concentrations at 10 °C are 0.3−0.6 and 10−14 M, respectively. The reaction time can be extended to 60 min. At the higher temperature of 40 °C, the etching reaction became so violent that the SiNWs were easy to be overetched. Therefore, the concentration of etchants and reaction time should be decreased. The appropriate H_2O_2 and HF concentrations are therefore 0.15−0.25 and 7−9 M, respectively. The etching time is suggested to be less than 30 min.

3.5. TEM and *I*−*V* Measurements. TEM and high-resolution TEM (HRTEM) were used to study the crystalline structure of the SiNWs. The as-prepared SiNWs were scratched off the substrate and dispersed in ethanol. After 10 s of sonication, several drops of the suspension were placed on a grid structure. Then, the grid was dried at room temperature and loaded into the TEM system. Figure 6a,b shows TEM and HRTEM images of the as-prepared SiNWs formed in the etching solution containing 8 M HF and 0.4 M H_2O_2 at 25 °C for 15 min. The inset in Figure 6b is the fast Fourier transform (FFT) pattern of the corresponding lattice-resolved HRTEM image. As shown in Figure 6a, the diffractive strips of SiNWs are clear, indicating that the SiNWs were crystals. The FFT pattern (Figure 6b) combined with the crystal lattice image revealed that the SiNWs had a [100] direction, which agrees well with the corresponding cross-sectional SEM image shown in Figure 6c.

Two-terminal *I*−*V* measurements were performed on an individual SiNW to investigate its electron-transport behavior. Measurement electrodes were made by electron-beam-evaporated Ti/Pt/Au 80 nm/50 nm/150 nm on a 200-nm SiO_2-coated silicon sample. The SiNWs were sonicated off the substrate in ethanol. Then, several drops of SiNW suspension were placed on the measurement electrodes and dried with a N_2 flow. The test structure is shown in Figure 7a. From this SEM image, it can be seen that the SiNW had a diameter of 290 nm, and the length between the two measurement electrodes was 880 nm. We assumed that the SiNW was cylindrical and had the same resistivity of 0.0035 Ω·cm as the Si wafer used. Based on Ohm's law, the resistance of the SiNW was estimated to be 466 Ω. However, the actual resistance was much larger than the estimated value. Figure 7b shows the measured current as a function of voltage ranging from −1 to 1 V. The *I*−*V* curve was nonlinear, indicating that the contact was slightly nonohmic. This can be explained by the fact that there existed two Schottky barriers connected back to back at the two sides of SiNW.[19] At low bias, few electrons had enough energy to overcome the barrier height, resulting in a low current. When the bias was increased to be greater than 0.5 V, the *I*−*V* curve became almost linear. In this large-bias regime, the resistance of the SiNW could be obtained by directly differentiating the *I*−*V* curve.[20,21] The calculated resistance was about ∼10^5 Ω, which was much larger than the resistance value of 466 Ω estimated from the resistivity of the Si wafer used. The greatly increased resistance could be due to several factors: (1) The etching reaction preferentially removed the dopants, so the overall doping concentration could be reduced.[13] (2) The contact at the interface of the measurement electrode and SiNW was nonideal because of its rough surface and small contact area. (3) A native oxide layer existed on the surface of SiNW,[22] which reduced the current-conducting volume. Further exploration of this *I*−*V* character and ohmic contact between the SiNW and metal electrode is still under investigation.

4. CONCLUSIONS

In summary, the synthesis of heavily doped SiNWs using a silver-assisted chemical etching method has been systematically investigated. The effects of H_2O_2 and HF concentrations,

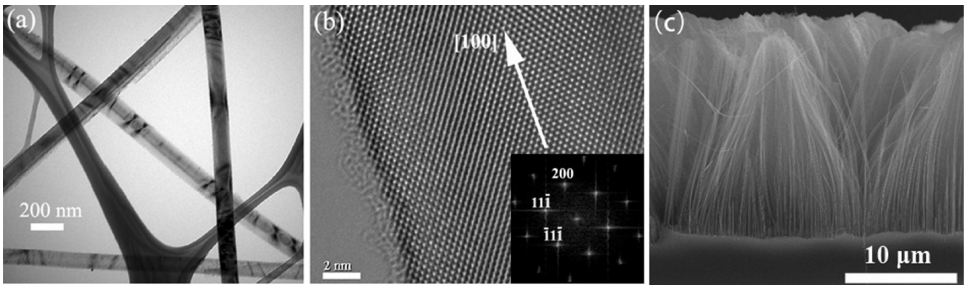

Figure 6. (a) TEM, (b) HRTEM, and (c) cross-sectional SEM images of the as-prepared SiNWs in the etching solution containing 8 M HF and 0.4 M H_2O_2 at 25 °C for 15 min.

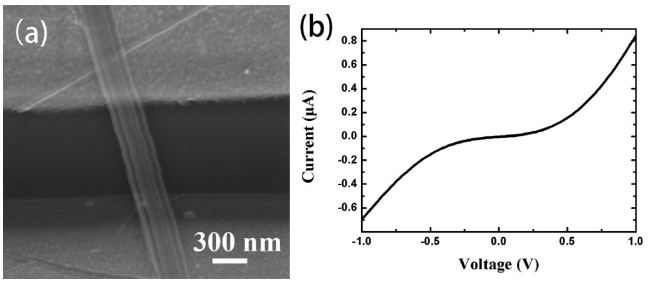

Figure 7. (a) Top-view SEM image of the *I*–*V* test structure. (b) *I*–*V* measurement curve recorded on a single SiNW with a diameter of about 290 nm and a length of about 880 nm.

reaction temperature, and etching time were discussed based on an electron-transfer model, and a chemical etching processing window was proposed. When the reaction temperature is controlled at room temperature, the reaction time should be less than 40 min. The appropriate range of H_2O_2 concentrations is 0.2–0.4 M, and the corresponding range of HF concentrations is 8–10 M. In addition, the H_2O_2 and HF concentrations should be varied slightly with changing temperature. These parameters provide a clear processing window for obtaining high-quality heavily doped SiNWs using the MACE method.

AUTHOR INFORMATION

Corresponding Author

*Tel.: +86-10-82305042. Fax: +86-10-82305141. E-mail: xdwang@semi.ac.cn.

Notes

The authors declare no competing financial interest.

ACKNOWLEDGMENTS

The authors gratefully acknowledge the support from the National Natural Science Foundation of China under Grants 61076077 and 61274066 and the National Basic Research Program of China (973 Program) under Grant 2012CB934204.

REFERENCES

(1) Boukai, A. I.; Bunimovich, Y.; Tahir-Kheli, J.; Yu, J. K.; Goddard, W. A.; Heath, J. R. Silicon Nanowires as Efficient Thermoelectric Materials. *Nature* **2008**, *451*, 168–171.

(2) Cui, Y.; Zhong, Z.; Wang, D.; Wang, W. U.; Lieber, C. M. High Performance Silicon Nanowire Field Effect Transistors. *Nano Lett.* **2003**, *3*, 149–152.

(3) Lee, S.-Y.; Jang, C.-O.; Kim, D.-J.; Hyung, J.-H.; Rogdakis, K.; Bano, E.; Zekentes, K.; Lee, S.-K. Fabrication of Ion-Implanted Si Nanowire p-FETs. *J. Phys. Chem. C* **2008**, *112*, 13287–13291.

(4) Tian, B.; Zheng, X.; Kempa, T. J.; Fang, Y.; Yu, N.; Yu, G.; Huang, J.; Lieber, C. M. Coaxial Silicon Nanowires as Solar Cells and Nanoelectronic Power Sources. *Nature* **2007**, *449*, 885–889.

(5) Chan, C. K.; Peng, H.; Liu, G.; McIlwrath, K.; Zhang, X. F.; Huggins, R. A.; Cui, Y. High-Performance Lithium Battery Anodes Using Silicon Nanowires. *Nat. Nanotechnol.* **2007**, *3*, 31–35.

(6) Ruffo, R.; Hong, S. S.; Chan, C. K.; Huggins, R. A.; Cui, Y. Impedance Analysis of Silicon Nanowire Lithium Ion Battery Anodes. *J. Phys. Chem. C* **2009**, *113*, 11390–11398.

(7) Hochbaum, A. I.; Chen, R. K.; Delgado, R. D.; Liang, W. J.; Garnett, E. C.; Najarian, M.; Majumdar, A.; Yang, P. D. Enhanced Thermoelectric Performance of Rough Silicon Nanowires. *Nature* **2008**, *451*, 163–167.

(8) Qu, Y.; Zhong, X.; Li, Y.; Liao, L.; Huang, Y.; Duan, X. Photocatalytic Properties of Porous Silicon Nanowires. *J. Mater. Chem.* **2010**, *20*, 3590–3594.

(9) Peng, K.; Yan, Y.; Gao, S.; Zhu, J. Dendrite-Assisted Growth of Silicon Nanowires in Electroless Metal Deposition. *Adv. Funct. Mater.* **2003**, *13*, 127–132.

(10) Geyer, N.; Huang, Z.; Fuhrmann, B.; Grimm, S.; Reiche, M.; Nguyen-Duc, T.-K.; de Boor, J.; Leipner, H. S.; Werner, P.; Gösele, U. Sub-20 nm Si/Ge Superlattice Nanowires by Metal-Assisted Etching. *Nano Lett.* **2009**, *9*, 3106–3110.

(11) Huang, Z.; Geyer, N.; Werner, P.; de Boor, J.; Gösele, U. Metal-Assisted Chemical Etching of Silicon: A Review. *Adv. Mater.* **2011**, *23*, 285–308.

(12) Chen, C.-Y.; Wu, C.-S.; Chou, C.-J.; Yen, T.-J. Morphological Control of Single-Crystalline Silicon Nanowire Arrays near Room Temperature. *Adv. Mater.* **2008**, *20*, 3811–3815.

(13) Qu, Y.; Liao, L.; Li, Y.; Zhang, H.; Huang, Y.; Duan, X. Electrically Conductive and Optically Active Porous Silicon Nanowires. *Nano Lett.* **2009**, *9*, 4539–4543.

(14) Oskam, G.; Long, J.; Natarajan, A.; Searson, P. Electrochemical Deposition of Metals Onto Silicon. *J. Phys. D: Appl. Phys.* **1998**, *31*, 1927–1949.

(15) To, W. K.; Tsang, C. H.; Li, H. H.; Huang, Z. Fabrication of n-Type Mesoporous Silicon Nanowires by One-Step Etching. *Nano Lett.* **2011**, *11*, 5252–5258.

(16) Zhang, M. L.; Peng, K. Q.; Fan, X.; Jie, J. S.; Zhang, R. Q.; Lee, S. T.; Wong, N. B. Preparation of Large-Area Uniform Silicon Nanowires Arrays through Metal-Assisted Chemical Etching. *J. Phys. Chem. C* **2008**, *112*, 4444–4450.

(17) Zhong, X.; Qu, Y.; Lin, Y. C.; Liao, L.; Duan, X. Unveiling the Formation Pathway of Single Crystalline Porous Silicon Nanowires. *ACS Appl. Mater. Interfaces* **2011**, *3*, 261–270.

(18) Cheng, S. L.; Chung, C. H.; Lee, H. C. A Study of the Synthesis, Characterization, and Kinetics of Vertical Silicon Nanowire Arrays on (001)Si Substrates. *J. Electrochem. Soc.* **2008**, *155*, D711–D714.

(19) Ke, J. J.; Tsai, K. T.; Dai, Y. A.; He, J. H. Contact Transport of Focused Ion Beam-Deposited Pt to Si Nanowires: From Measurement to Understanding. *Appl. Phys. Lett.* **2012**, *100*, 053503.

(20) Zhang, Z. Y.; Jin, C. H.; Liang, X. L.; Chen, Q.; Peng, L. M. Current–Voltage Characteristics and Parameter Retrieval of Semiconducting Nanowires. *Appl. Phys. Lett.* **2006**, *88*, 073102.

(21) Zhang, Z.; Yao, K.; Liu, Y.; Jin, C.; Liang, X.; Chen, Q.; Peng, L. M. Quantitative Analysis of Current−Voltage Characteristics of Semiconducting Nanowires: Decoupling of Contact Effects. *Adv. Funct. Mater.* **2007**, *17*, 2478−2489.
(22) Cui, Y.; Duan, X.; Hu, J.; Lieber, C. M. Doping and Electrical Transport in Silicon Nanowires. *J. Phys. Chem. B* **2000**, *104*, 5213−5216.